Immunoprofiles and Treatment Strategies for Molecular Subtypes of Endometrial Cancer

Kim, Jung Chul

Department of Medicine
Graduate School
Yonsei University

Immunoprofiles and Treatment Strategies for Molecular Subtypes of Endometrial Cancer

Advisor Lee, Jung-Yun

A Dissertation Submitted
to the Department of Medicine
and the Committee on Graduate School
of Yonsei University in Partial Fulfillment of the
Requirements for the degree of
Doctor of Philosophy in Medical Science

Kim, Jung Chul

July 2025

Immunoprofiles and Treatment Strategies for Molecular Subtypes of Endometrial Cancer

This certifies that the Dissertation of Kim, Jung Chul is approved

Thesis Supervisor	Lee, Jung-Yun
Thesis Committee Member	Lee, Seung-Tae
Thesis Committee Member	Chang, Suhwan
Thesis Committee Member	Kim, Hyun-Soo
Thesis Committee Member	Park, Junsik

Department of Medicine
Graduate School
Yonsei University

December 2024

ACKNOWLEDGEMENTS

Throughout my doctoral journey, I have been fortunate to receive the invaluable support of several individuals who helped me complete my thesis successfully.

I would like to take this opportunity to express my heartfelt gratitude. I am deeply thankful to Professor Jung-Yun Lee for offering fresh perspectives on my research and guiding me in formulating a comprehensive plan for its completion. The mentorship of the professor has enabled me to conduct meaningful research and share my experiences, making this an incredibly rewarding learning process.

I also extend my sincere thanks to Professors Junsik Park, Hyun-Soo Kim, Suhwan Chang, and Seung-Tae Lee for their generous commitment to thoroughly reviewing my paper despite their demanding schedules. Reflecting on my doctoral journey, I recall the countless challenges in balancing hospital duties, graduate studies, and my research. Despite these obstacles, I take pride in the dedication and perseverance I invested in this pivotal period of my life.

While it is not possible to name everyone individually, I would like to express my deep appreciation to all those who have supported, encouraged, and believed in me throughout this journey. Moving forward, I remain committed to refining my skills and contributing meaningfully to the medical field by embodying a vision of growth, purpose, and excellence.

TABLE OF CONTENTS

LIST OF FIGURES

LIST OF TABLES

ABSTRACT

Immunoprofiles and Treatment Strategies for Molecular Subtypes of Endometrial Cancer

Purpose:

Understanding of immune profiles across endometrial cancer (EC) subtypes and the impact of specific molecular markers on immune responses and their therapeutic implications remain limited. This study aimed to assess the immune profiles of EC subtypes based on the Proactive Molecular Risk Classifier for Endometrial Cancer (ProMisE) classification and evaluate the impact of specific molecular markers, such as L1 cell adhesion molecule (L1CAM), AT-rich interaction domain 1A (*ARID1A*), and different mismatch repair (MMR) protein deficiencies, on the immune response and therapeutic potential.

Methods:

Patients with treatment-naïve EC from Severance Hospital (2019–2023) were included. Polymerase-ε (POLE) mutations were detected using droplet digital polymerase chain reaction, and immunohistochemistry was used to assess the expression of p53, MMR proteins (MSH6, PMS2, MSH2, and MLH1), L1CAM, and *ARID1A*. Tumor-infiltrating lymphocytes (TILs) were analyzed using flow cytometry to identify various immune cell subsets and their functional states, including CD8+ T cells, regulatory T cells, and markers of T cell exhaustion or activation.

Results:

Immune profiles varied across EC subtypes. The POLE-mutated and MMR-deficient (MMRd) subtype tumors showed strong immune responses, however, with signs of exhaustion, including high PD-1 and TOX expression, suggesting sensitivity to immune checkpoint inhibitors. The no specific molecular profile (NSMP) and p53-abnormal subtypes showed lower immune cell infiltration and more immunosuppressive environments. Among MMRd tumors, those with MSH2/MSH6 deficiency demonstrated greater $CD8^+$ T cell infiltration than MLH1/PMS2-deficient tumors,

implying a more robust immune activation profile. In the NSMP subtype, L1CAM-positive tumors showed increased levels of markers of T cell exhaustion, including PD-1 and TIGIT, whereas *ARID1A*-negative tumors showed a greater proportion of tumor-reactive CD8+ T cells (CD103+CD39+), indicating the potential for enhanced immune surveillance, although some signs of exhaustion were present.

Conclusion:

This study highlights the importance of the molecular subtyping of ECs in guiding personalized immunotherapy strategies. The POLE-mutated and MMRd subtype tumors exhibited robust immune responses; however, indicators of exhaustion were also observed, implying their potential responsiveness to immune checkpoint inhibitors. In addition, MSH2/MSH6-deficient tumors, as well as L1CAM-positive and ARID1A-negative tumors within the NSMP subgroup, were identified as potential targets for therapeutic strategies aimed at reversing immune exhaustion and enhancing treatment efficacy.

Key words : Endometrial cancer; Molecular subtype; Tumor infiltrating lymphocyte

1. INTRODUCTION

Endometrial cancer (EC) is the most prevalent gynecological malignancy in postmenopausal women in developed nations, with its incidence rising due to the growing prevalence of obesity and an aging population [1]. The number of EC cases in Korea has also increased, from 728 in 1999 to 3749 in 2021. Of these, 30.5% of the patients were in their 50s, 18.7% in 40s, and 25.8% in 60s [2].

EC is often detected at an early stage owing to symptoms, such as abnormal vaginal bleeding, with the development of various imaging diagnostic tools and relatively straightforward diagnostic methods [3]. Consequently, among different types of cancers, EC is associated with relatively low mortality rates. The treatment approaches for EC are currently tailored based on risk factors, such as the International Federation of Gynecology and Obstetrics (FIGO) stage, grade, clinicopathological features, age, extent of myometrial invasion, and the presence or absence of lymphovascular space invasion (LVSI) [4]. However, after the publication of four novel molecular risk factors in EC by The Cancer Genome Atlas (TCGA) group in 2013, a clinically easy-to-use molecular classification system named Proactive Molecular Risk Classifier for Endometrial Cancer (ProMisE) emerged. This system, which uses immunohistochemical (IHC) stains—p53 and mismatch repair (MMR) proteins—and polymerase-ε (POLE) exonuclease domain hotspot sequencing as the surrogate marker, was validated by research groups in the Netherlands and Vancouver [5, 6]. The differences in survival rates among the molecular subtypes were reported in the PORTEC-2 study, leading to studies investigating whether molecular subtypes can guide adjuvant treatment strategies and the reasons underpinning these differences [7].

Molecular subtypes of EC exhibit immunological differences in the tumor microenvironment caused by endogenous DNA repair defects. Specifically, POLE-mutated tumor subtypes are ultramutated (mean = 232×10^{-6} mutations/Mb), and mismatch repair-deficient (MMRd) tumors are hypermutated (18×10^{-6} mutations/Mb) [8, 9]. Hence, these mutations are assumed to induce an antitumor immune response by activating the tumor-infiltrating lymphocyte (TIL) response through a high neoantigen load.

The clinical application of immune checkpoint inhibitors (ICIs), which promote anti-tumor immune responses in EC cases characterized by MMRd or high microsatellite instability (MSI-H), has shown increasing effectiveness. Although MSI-H accounts for 20–30% of EC cases, only

approximately 50% of them respond to ICI therapy [9]. Additionally, re-administration of ICIs after recurrence is increasingly being considered in gynecological and solid tumors [10], highlighting their clinical significance and the need to identify responsive patient groups and understand the immunological properties of EC.

The surface antigen characteristics of EC subtypes and tumor-infiltrating immune cells have been explored previously. However, these studies were limited by the methods used for the analysis of the characteristic expression patterns, such as IHC for the identification of tumor-infiltrating immune cells. Furthermore, studies on emerging markers, such as L1 cell adhesion molecule (L1CAM) and AT-rich interaction domain 1A (*ARID1A*) in EC are lacking.

ARID1A deficiency is associated with enhanced infiltration of immune cells, especially TILs, across various cancer types [11, 12]. Tumors with *ARID1A* mutations typically show increased levels of TILs and heightened activity of immune checkpoints, such as PD-1/PD-L1. This leads to an increased immunogenic tumor environment, potentially improving the response to ICIs, such as anti-PD-1/PD-L1 therapies. For example, research on lung adenocarcinoma and hepatocellular carcinoma has shown that *ARID1A* mutations facilitate TIL infiltration, activate immune-related pathways such as STING-mediated responses, and improve patient survival in the context of ICI treatment [13].

In contrast, L1CAM is involved in promoting tumor progression and immune evasion. In ovarian carcinoma, L1CAM contributes to an immunosuppressive environment and poor prognosis by promoting tumor cell motility, invasion, and stemness [14, 15]. Tumors with high L1CAM expression typically exhibit reduced infiltration of immune cells, particularly cytotoxic T cells, allowing for increased immune evasion and resistance to immune-based therapies, such as checkpoint inhibitors [16].

Therefore, to elucidate the immune landscape of endometrial cancer, we aimed to comprehensively characterize TILs according to the established molecular subtypes as well as emerging immunoregulatory markers. We employed fluorescence-activated cell sorting (FACS), a robust technique for high-resolution immunophenotyping at the single-cell level, which enables precise identification of surface antigen expression and delineation of T cell subsets, including functionally distinct populations of $CD8^+$ TILs. Through this approach, we sought to define subtype-specific immune signatures and uncover potential immunologic targets for future therapeutic interventions.

2. MATERIALS AND METHODS

2-1. Study participant selection and lymphocyte isolation

Tumor samples from patients with EC were collected from 2019 to 2023 at Severance Hospital Obstetrics and Gynecology based on the sample collected with "부인암 환자 유래 오가노이드를 이용한 맞춤치료 모델 개발 (CR no. 4-2018-0928)." We analyzed the clinical and pathological data of patients at all stages of treatment-naïve EC, including MMR status (MSH6, PMS2, MSH-2, and MLH-1) determined using IHC and p53 abnormality data (Figure 1).

Fresh tumor tissues were obtained on the day of surgical resection for translational research. To obtain single-cell suspensions, the tumor tissues were mechanically and enzymatically dissociated using a tumor dissociation kit (Miltenyi Biotec, 130-095-929) as per the manufacturer's guidelines. The suspensions were filtered through a 100μm cell strainer to remove debris and were cryopreserved for future experimental applications.

2-2. Bulk RNA sequencing

Bulk RNA sequencing of some EC tissue samples was performed as follows. Formalin-fixed paraffin-embedded (FFPE) tissue sections were prepared and RNA was extracted using a standardized protocol optimized for FFPE samples. The extracted RNA was quantified and assessed for quality using spectrophotometry with a bioanalyzer system to ensure sufficient integrity for sequencing. Library preparation included the reverse transcription of RNA into cDNA, followed by fragmentation, adapter ligation, and amplification. High-throughput sequencing was performed on an Illumina platform. The resulting raw sequencing data were subjected to quality control, including trimming of low-quality bases and removal of adapter sequences. RNA-Seq data were analyzed using Basepair software (https://www.basepairtech.com/). Specifically, using STAR with default parameters, the reads were aligned to the transcriptome based on the UCSC genome assembly hg19 [17]. The featureCounts was used to quantify the read counts for each transcript [18]. DESeq2 was employed to identify differentially expressed genes, applying thresholds of read count > 10 and $p < 0.01$ for pathway and target gene analyses.

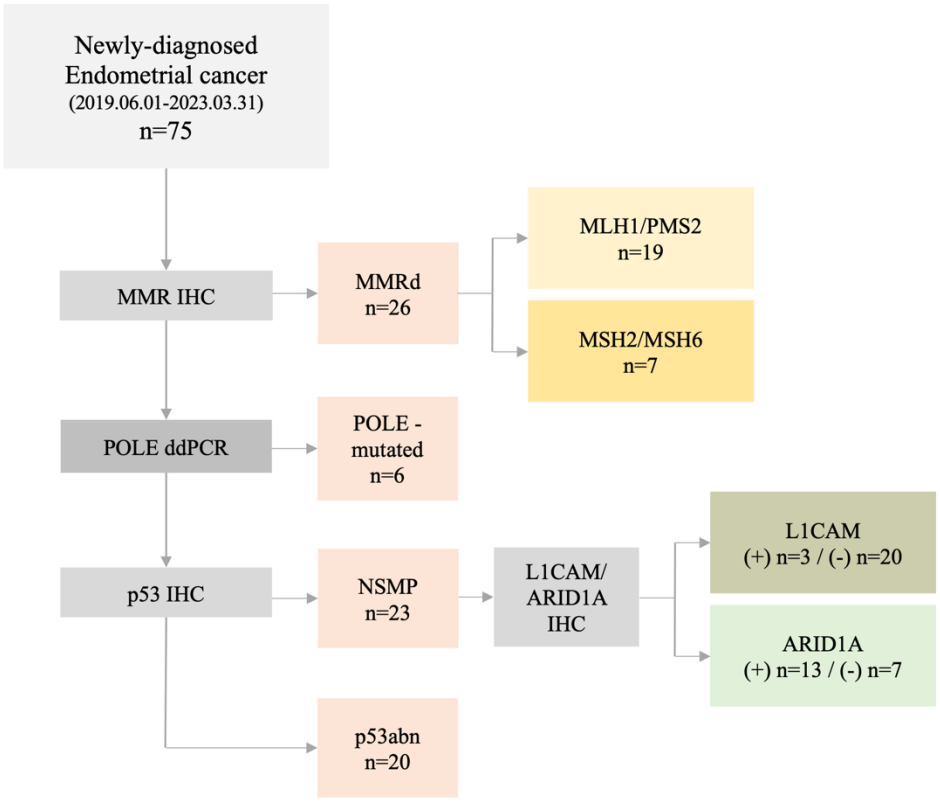

Figure 1. Schematic of the study.

2-3. POLE mutation detection and L1CAM and *ARID1A* expression analyses

To detect POLE mutations, FFPE EC tissue samples were sectioned and DNA was extracted using the QIAamp® DSP DNA FFPE tissue kit. DNA was quantified using NanoDrop analysis and tested using droplet digital polymerase chain reaction (ddPCR) with the Droplex POLE mutation test, targeting mutations in exons 9, 13, and 14. The QX200™ Droplet Digital PCR system, known for its high sensitivity and specificity, was utilized, and data were processed using QuantaSoft™ software with appropriate controls to maintain accuracy. This approach allowed for precise identification of POLE mutations in minimal DNA samples, ensuring dependable diagnostics.

The expression levels of L1CAM and *ARID1A* in EC tissues were evaluated using IHC. FFPE tissue sections were prepared and deparaffinized. With antigen retrieval, sections were incubated with primary antibodies specific for L1CAM and *ARID1A*. The slides were treated with an enzyme-conjugated secondary antibody, followed by chromogen development for visualization. Hematoxylin was used as the counterstain. The stained slides were examined under a microscope and the expression levels were scored based on the intensity and proportion of positive cells. For L1CAM, IHC staining was assessed as positive when ≥ 10% of tumor cells showed strong membranous staining and staining intensity was evaluated using a semi-quantitative scoring system. For *ARID1A*, nuclear staining in tumor cells was defined as positive. The loss of *ARID1A* expression was identified by the lack of nuclear staining in tumor cells, while stromal cells and neighboring normal tissues acted as internal positive controls for both markers.

2-4. Flow cytometry

Cryopreserved TILs and peripheral blood mononuclear cells (PBMCs) were prepared and stained with fluorochrome-conjugated antibodies against markers such as CD3, CD4, CD8, CD45, CD45RA, FoxP3 and CCR7. Live/dead discrimination was performed using the LIVE/DEAD Fixable Near IR Cell Stain Kit (Life Technologies, Carlsbad, California, USA) to exclude non-viable CD45+ cells from the analysis. Subsequent gating identified CD3+ T cells, followed by further analysis distinguishing between CD4+ and CD8+ subsets. Within the CD4+ population, regulatory T cells (FoxP3+) and memory/effector subsets (CD45RA and CCR7) were characterized. The proportions and phenotypes of these immune cell subsets were determined to assess their functional roles. CXCR5 and PD-1 were used to characterize follicular helper T cells (Tfh) and exhausted T cells,

respectively. T cell exhaustion markers, namely, TIGIT and TIM-3, and tumor-reactive T cell-associated markers CD39 and CD103 were also analyzed. CD226, a co-stimulatory receptor, was assessed alongside TIGIT to evaluate opposing roles in immune regulation. CTLA-4 expression was measured as an indicator of T cell inhibition and immunosuppressive activity, whereas 4-1BB, a co-stimulatory molecule, was analyzed to identify activated and proliferating T cells. Ki-67 was used to gauge T cell proliferation rates. TCF-1 expression was used to identify less-exhausted and potentially functional T cells, whereas TOX was evaluated as a marker of deep T cell exhaustion. LAG-3, another checkpoint receptor, was examined for its role in suppressing T cell activity. Finally, the chemokine receptors CCR8 and CCR4 were assessed to determine the presence of regulatory T cells (Tregs) involved in shaping the immunosuppressive tumor microenvironment. Multicolor flow cytometry was performed using a BD FACSLylic system (BD Biosciences, San Jose, California, USA). Data were analyzed using FlowJo software V.10.8 (BD Life Sciences) (flowjo. com).

2-5. In vitro T cell proliferation assay

We performed an in vitro T cell proliferation assay to compare the reinvigoration ability of exhausted CD8+ TILs after anti-PD-1 (aPD-1) treatment with or without anti-CTLA-4 (aCTLA-4) treatment. Cryopreserved TILs were thawed, suspended in RPMI 1640 medium containing 10% fetal bovine serum and incubated for 8 h at 37°C under 5% CO_2. TILs were labeled with CellTrace Violet (CTV; Thermo Fisher Scientific). A total of 100,000 cells were plated in 200 μL of medium per well in a 96-well round-bottom culture plate; the cells were stimulated using soluble anti-CD3 antibody (10 ng/mL, OKT-3; BD Bioscience) in the presence of isotype control (mIgG1, MOPC-21; BioLegend), 5 μg/mL aPD-1 (EH12.2H7), or 5 μg/mL aPD-1 with 5 μg/mL aCTLA-4. The cells were harvested after 96 h of culture in a 5% CO_2 incubator, and CTVlowCD8+ T cells were counted as proliferated cells; the fold change in CTVlowCD8+ T cells was calculated relative to the isotype control.

2-6. Statistical analysis

Demographic data were presented using descriptive statistics, with continuous variables summarized as medians (ranges) and categorical variables as frequencies (percentages). The D'Agostino and Pearson omnibus test was employed to assess the normality of the continuous variables. The unpaired t-test or the Mann–Whitney U test, depending on the distribution of the data,

was used to compare continuous variables, whereas categorical variables were evaluated using the Pearson χ^2 test. Overall survival (OS) and progression-free survival (PFS) were estimated using the Kaplan–Meier method, and differences were assessed using log-rank tests. Statistical analyses were performed using Prism software version 8 (GraphPad Software, San Diego, CA, USA), SPSS software version 27 (IBM), or R version 4.0.3 (R Foundation for Statistical Computing, Vienna, Austria). Statistical significance was set at $p < 0.05$.

3. RESULTS

3-1. Distinct clinicopathologic characteristics and survival outcomes across ProMisE molecular subtypes

Significant differences in age, menopausal status, and histological subtypes were observed in the baseline demographics and clinicopathological characteristics of patients stratified by ProMisE molecular subtypes (Table 1). The p53-abnormal (p53abn) group was the oldest (mean age 64.1 years, p = 0.012) and had the highest proportion of patients who attained menopause (85.0%; p = 0.021). Endometrioid carcinoma was predominant in the no specific molecular profile (NSMP) (95.7%) and MMRd (88.5%) groups, whereas serous carcinoma was unique to the p53abn group (30.0%). The POLE mutation group was diverse and included patients with carcinosarcoma (33.3%). Survival analysis showed that while the median PFS for the NSMP group was 43.13 months, the other groups did not reach the median PFS, although the difference was not statistically significant (p = 0.1984) (Figure 2A, 2B). Similarly, OS was not reached across all groups (p = 0.3707).

3-2. Bulk RNA sequencing of EC subtypes reveals strong immune activity in POLE-mutated and MMRd tumors

Bulk RNA sequencing analysis of some EC tissues classified by molecular subtype revealed distinct immune signatures associated with each group (Figure 2C–2E). POLE-mutated and MMRd (n= 6, 3) tumors demonstrated strong enrichment of cytotoxic markers, such as CD8A, GZMK, and TBX21. Exhaustion markers, such as PDCD1, TOX, CTLA4, TIGIT, and ENTPD-1, were also highly expressed in these tumors suggesting a robust, however, potentially exhausted immune environment. The NSMP & p53abn tumors (MMR-proficient [MMRp] marked, n=5) showed the lowest immune activity with lower expression levels of key immune markers and a relatively immunosuppressive profile, as highlighted by elevated L1CAM. Statistical analysis confirmed the differential expression patterns, with POLE-mutated and MMRd tumors showing negative enrichment (p = 0.002) in DNA repair groups and positive enrichment (p = 0.076) in Tregs (GSE14415). These results aligned with the FACS data identifying specific T cell subsets and their functional states. For example, elevated PD-1 expression identified via RNA sequencing was corroborated by the presence of increased PD-1+CD8+ T cells observed through flow cytometry.

Table 1. Baseline demographics and characteristics of the study population.

	POLE-mutated (N = 6)	MMRd (N = 26)	NSMP (N = 23)	p53abn (N = 20)	Total (N = 75)	p value
Age (year)						
Mean (SD)	54.7 (±12.4)	53.5 (±9.7)	54.4 (±12.1)	64.1 (±12.2)	56.7 (±12.0)	0.012
BMI						
Mean (SD)	23.7(±5.1)	24.8(±7.1)	28.0(±8.2)	24.7(±6.0)	25.7 (±7.1)	0.313
Parity						
0	2 (33.3%)	6 (23.1%)	10 (43.5%)	4 (20.0%)	22 (29.3%)	0.308
1 or more	4 (66.7%)	20(76.9%)	13 (56.5%)	16 (80.0%)	53 (70.7%)	
Diabetes						
No	6 (100.0%)	21 (80.8%)	20 (87.0%)	16 (80.0%)	63 (84.0%)	0.630
Yes	0 (0.0%)	5 (19.2%)	3 (13.0%)	4 (20.0%)	12 (16.0%)	
Menopause						
No	4 (66.7%)	14 (53.8%)	12 (52.2%)	3 (15.0%)	33 (44.0%)	0.021
Yes	2 (33.3%)	12 (46.2%)	11 (47.8%)	17 (85.0%)	42 (56.0%)	
Prior malignancies						
No	6 (100.0%)	24 (92.3%)	21 (91.3%)	18 (90.0%)	69 (92.0%)	0.885
Yes	0 (0.0%)	2 (7.7%)	2 (8.7%)	2 (10.0%)	6 (8.0%)	
Histology						
Endometr-ioid	4 (66.7%)	23 (88.5%)	22 (95.7%)	7 (35.0%)	56 (74.7%)	<0.001
Serous	0 (0.0%)	0 (0.0%)	0 (0.0%)	6 (30.0%)	6 (8.0%)	
Clear cell	0 (0.0%)	1 (3.8%)	1 (4.3%)	3 (15.0%)	5 (6.7%)	
Mixed	0 (0.0%)	1 (3.8%)	0 (0.0%)	0 (0.0%)	1 (1.3%)	
Carcinosa-rcoma	2 (33.3%)	0 (0.0%)	0 (0.0%)	4 (20.0%)	6 (8.0%)	
Neuroend-ocrine	0 (0.0%)	1 (3.8%)	0 (0.0%)	0 (0.0%)	1 (1.3%)	
Stage at diagnosis						

I	6 (100.0%)	12 (46.2%)	10 (43.5%)	10 (50%)	38 (50.7%)	0.428
II	0 (0.0%)	4 (15.4%)	3 (13.0%)	1 (5.0%)	8 (10.7%)	
III	0 (0.0%)	8 (30.8%)	6 (26.1%)	7 (35.0%)	21 (28.0%)	
IV	0 (0.0%)	2 (7.7%)	4 (17.4%)	2 (10.0%)	8 (10.7%)	
Pathological grade						
1	1 (16.7%)	2 (7.7%)	4 (17.4%)	3 (15.0%)	10 (13.3%)	0.263
2	2 (33.3%)	16 (61.5%)	13 (56.5%)	5 (25.0%)	36 (48.0%)	
3	3 (50.0%)	6 (23.1%)	6 (26.1%)	11 (55.0%)	26 (34.7%)	
none	0 (0.0%)	2 (7.7%)	0 (0.0%)	1 (5.0%)	3 (4.0%)	
LVSI						
No	2 (33.3%)	13 (50.0%)	11 (47.8%)	10 (50.0%)	36 (48.0%)	0.898
Yes	4 (66.7%)	13 (50.0%)	12 (52.2%)	10 (50.0%)	39 (52.0%)	

SD, standard deviation; *LVSI*, lymph vascular space invasion

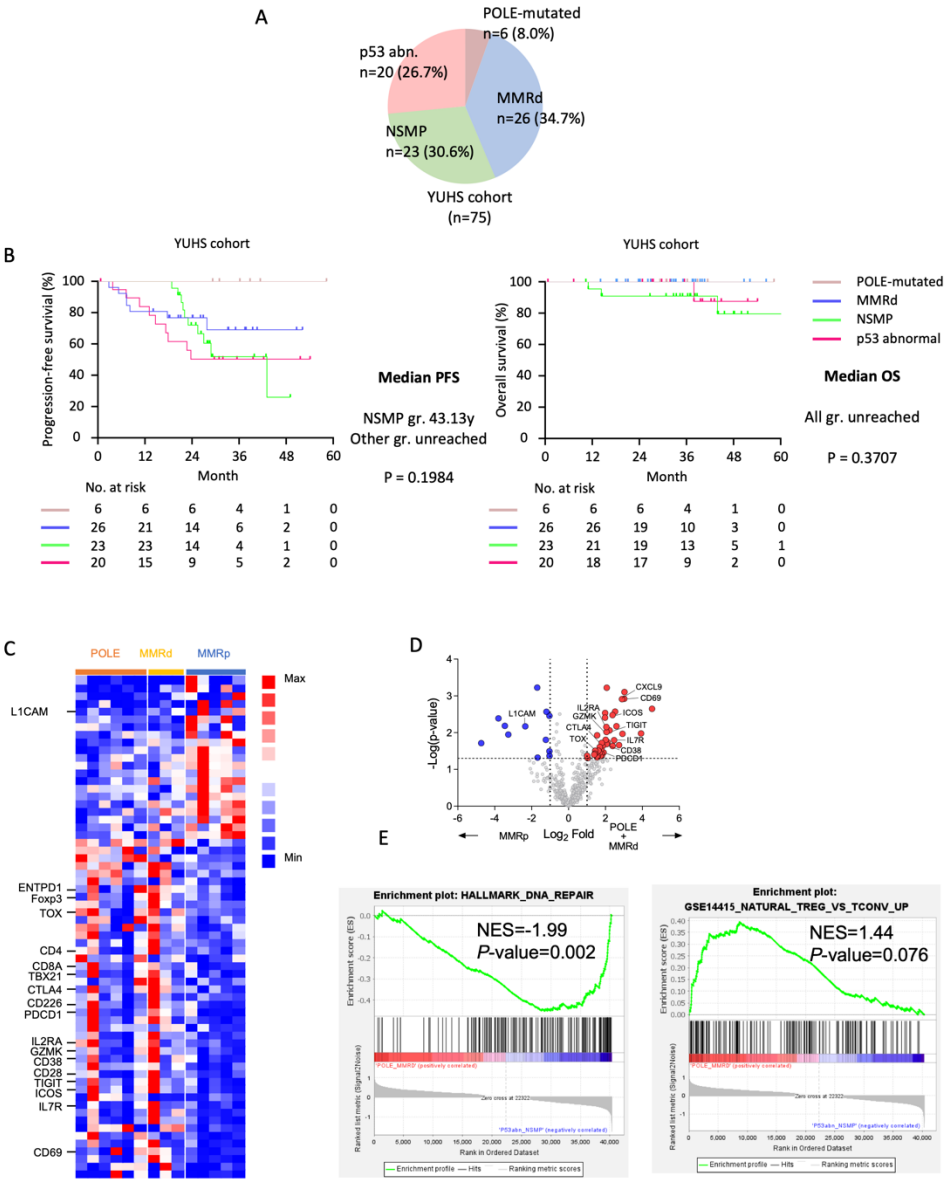

Figure 2. PFS and OS across molecular subtypes and differential expression of immune markers in bulk RNA sequencing. (A) The total number of patients in each molecular subtype. (B) PFS and OS. (C-E) Bulk RNA sequencing results of POLE-mutated & MMRd vs. NSMP & p53abn groups (MMRp marked). Immune exhausted genes (PDCD1, CTLA4, TIGIT, TOX, and ENTPD-1) were

upregulated in high mutational load group. Up-regulated gene sets in regulatory T cells (GSE14415) were enriched in POLE-mutated + MMRd groups.

Similarly, the presence of Tregs in RNA sequencing corresponded with elevated FoxP3+CD4+ Tregs in FACS analysis, highlighting an increased immunosuppressive environment in certain subtypes, such as MMRd tumors.

3-3. Subtype-specific immune profiles in EC highlight T cell infiltration, Treg-mediated immunosuppression, and T cell exhaustion across ProMisE classifications

Flow cytometry analysis delivered an in-depth characterization of TIL profiles, showcasing the distribution and functional state of immune cells in the tumor microenvironment. Lymphocytes were gated using singlets, live CD45+ cells, and CD3+ T cells. CD3+ cells were subdivided into CD4+ and CD8+ cell populations. Tregs were distinguished by the co-expression of CD4 and FoxP3. Memory subsets were characterized by CCR7 and CD45RA expression, whereas effector Tregs were identified based on CD45RA and FoxP3 expression (Figure 3). TILs exhibited a significant increase in the numbers of CD3+ and CD8+ T cells, indicating the presence of strong T cells in the tumor microenvironment. Elevated levels of FoxP3+CD4+ Tregs suggested an immunosuppressive environment, whereas increased levels of Tfh and CXCR5+PD-1+CD8+ T cells indicate potential T cell exhaustion. In addition, naïve, central memory, and effector memory CD8+ T cell subsets were more frequently observed in TILs, implying that the tumor may contribute to the retention of these cells (Figure 4). Flow cytometric analysis showed no significant differences in $CD45^+$, $CD3^+$ TILs, or regulatory T cell subsets across EC molecular subtypes. In contrast, POLE-mutated and MMRd tumors exhibited significantly higher proportions of effector memory $CD8^+$ T cells than p53-abnormal and NSMP tumors, suggesting enhanced cytotoxic potential in hypermutated subtypes. This may reflect active immune engagement but also sustained antigen exposure, potentially predisposing T cells to exhaustion. Other $CD8^+$ or $CD4^+$ subsets, including naïve, EMRA, and exhausted phenotypes, showed no notable differences. (Figure 5).

3-4. Distinct immune activation and exhaustion patterns in EC subtypes influence immunotherapy response

Within TILs, CD8+ T cells displayed significantly higher expression of PD-1, CD28, CD226, and

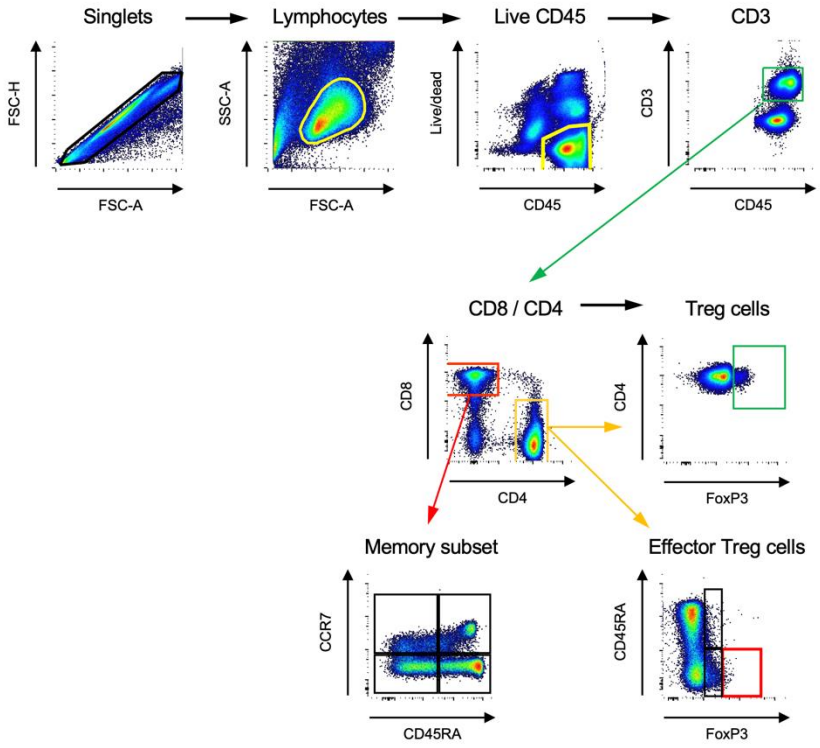

Figure 3. Gating strategy.

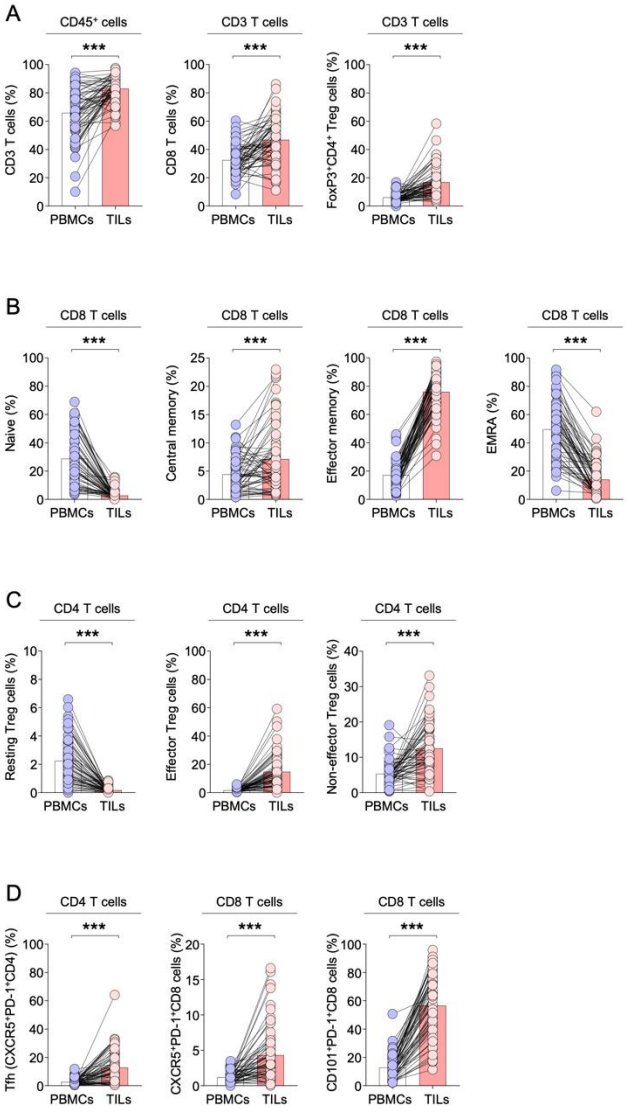

Figure 4. Cell composition in PBMCs and TILs. (A) Comparison of CD8+ and CD4+ T cells in PBMCs and TILs. (B) Distribution of effector memory T cells, memory T cells and EMRA in PBMCs and TILs. (C) Resting, effector, and non-effector Tregs subsets in PBMCs and TILs. (D) Tfh and CXCR5+PD-1+ and CD101+PD-1+ CD8+ T cells in PBMCs and TILs. ***p < 0.001; *EMRA*, effector memory cells re-expressing CD45RA.

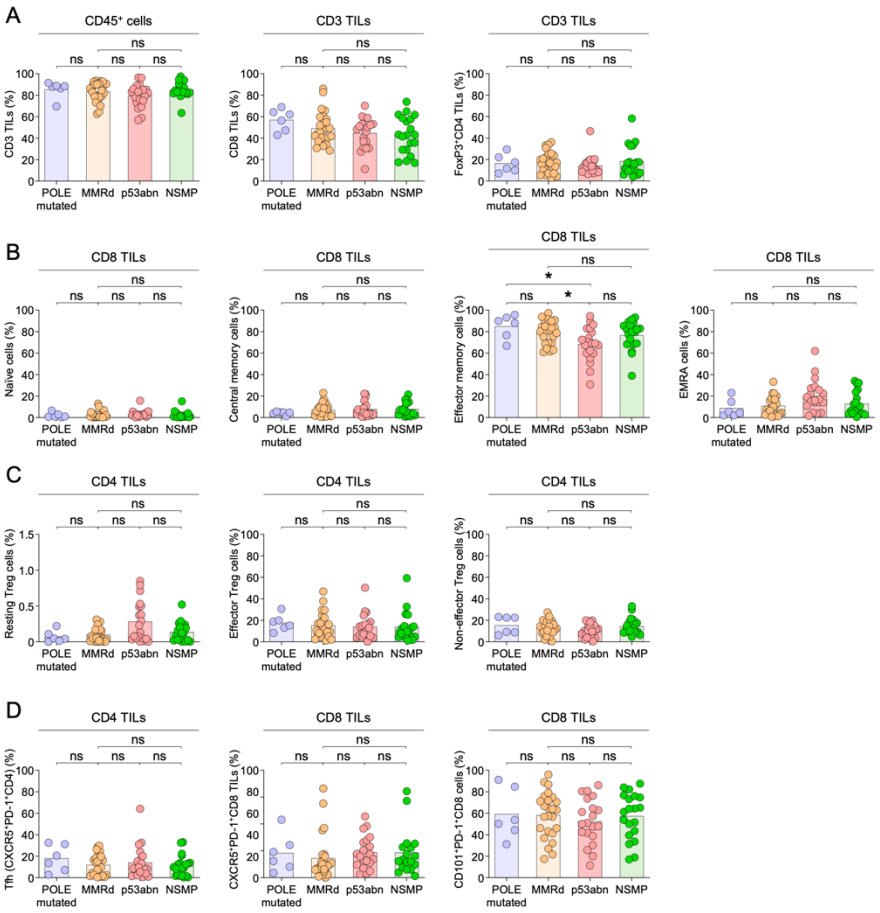

Figure 5. Cell composition of TILs according to ProMisE classifier. (A) Comparison of the proportions of CD8+ and CD4+ TILs across different molecular subtypes. (B) The distribution of effector Tregs and Tfh cells. (C) Comparison of memory T cell subsets. (D) Proportion of Tregs in these populations. *p < 0.05; **p < 0.01; ***p < 0.001; *ns*, not significant.

Ki-67 relative to PBMCs, suggesting enhanced activation and proliferation in the tumor microenvironment. Exhaustion markers, such as TIM-3, TOX, and TIGIT, were also elevated in the PD-1+CD8+ cell subset. This suggests a dual role for immune activation and exhaustion within the tumor, shaping a complex regulatory landscape that may affect therapeutic outcomes. These findings emphasize the distinct immunological environments of tumors and highlight the need to consider the tumor microenvironment in immunotherapy strategies (Figure 6). The distribution of immune markers across ProMisE subtypes revealed distinct immune environments. The POLE-mutated subtype showed elevated levels of TIM-3+, PD-1+, CD39+, TOX+ and CD103+CD39+ cells, indicating a highly active yet immunosuppressed environment caused by chronic activation and exhaustion. MMRd tumors also exhibited elevated CD39+ levels, indicating an active immune response with exhaustion. Conversely, the p53abn and NSMP subtypes displayed fewer elevations of these marker levels, suggesting a "cold" tumor microenvironment, potentially resistant to immune-based therapies. These findings suggest that the POLE-mutated and MMRd subtypes may respond better to ICIs, whereas p53abn and NSMP may require different therapeutic approaches (Figure 7).

3-5. Subtype-specific regulatory T cell suppression and exhaustion in EC tumors

Analysis of Tregs in TILs versus PBMCs revealed elevated expression of immune checkpoint markers such as PD-1, CTLA-4, and TIGIT in TILs, indicating a more suppressive and potentially exhausted environment around the tumor. Tumor Tregs exhibited increased levels of functional markers, such as Ki-67, CD39, and CCR8, reflecting active proliferation and enhanced immunosuppressive capacity. Additionally, 4-1BB+ Tregs, known for their strong suppressive function, were more pronounced in the tumor microenvironment (Figure 8). When stratified using the ProMisE classifier, POLE-mutated and MMRd subtypes had higher percentages of Tregs expressing PD-1 and CTLA-4, indicating a more suppressive immune environment. TIGIT expression was elevated in the MMRd group, further emphasizing the regulatory role of this subtype. These findings highlight molecular subtype-specific differences in Tregs behavior and underscore the potential for targeted immunotherapies tailored to these immune profiles (Figure 9).

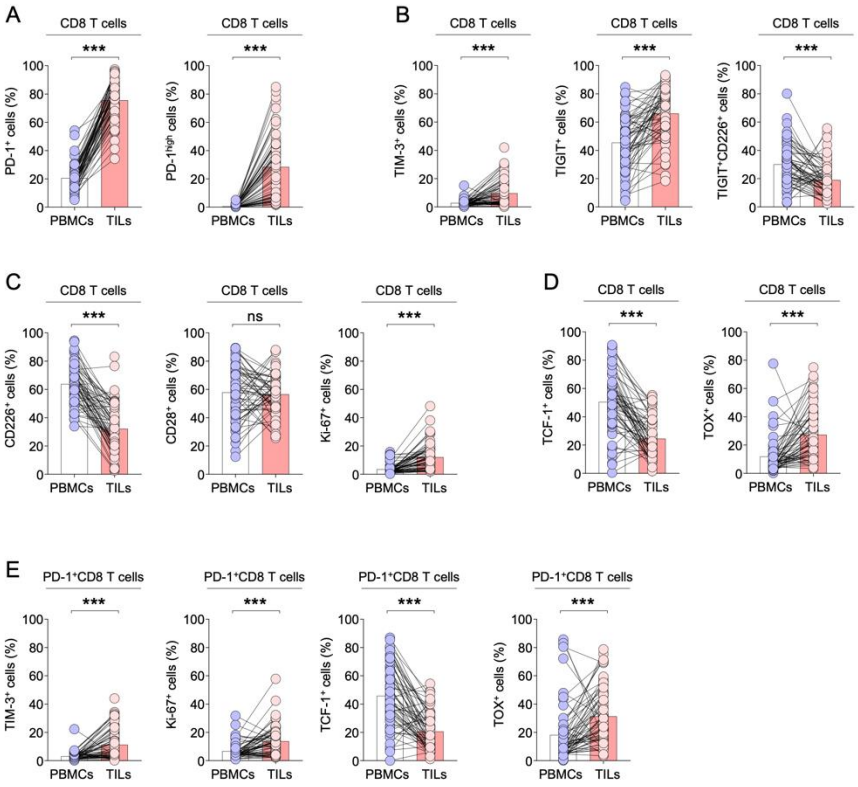

Figure 6. CD8+ T cells in PBMCs and TILs. (A) Comparison of PD-1+ and PD-1-high CD8+ T cells in PBMCs and TILs. (B) Expression of CD28+ and CD226+ CD8+ T cells in PBMCs and TILs. (C) Expression levels of proliferation markers TIM-3 and Ki-67 in PD-1+ CD8+ T cells. (D) TCF-1 and TOX expression in PD-1+ CD8+ T cells in PBMCs and TILs. (E) TIGIT+ and TIGIT+CD226+ CD8+ T cells in PBMCs and TILs. ***$p < 0.001$.

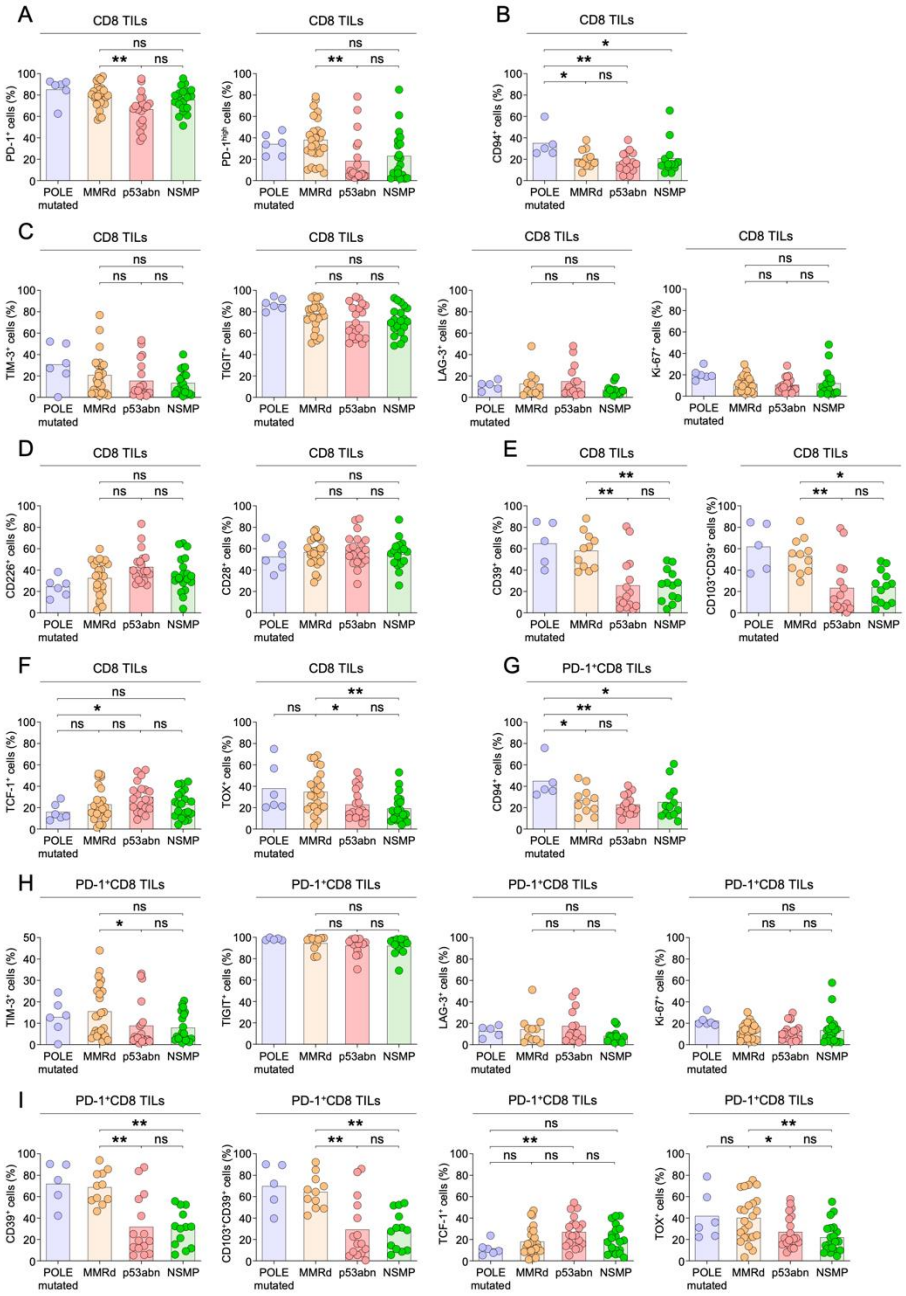

Figure 7. CD8+ TILs according to ProMisE classifier. (A-F) PD-1+, PD-1-high+, TIM-3+, TIGIT+, LAG-3+, Ki-67+, CD226+, CD28+, CD39+, CD103+CD39+, TCF-1+, and TOX+ cells in CD8+

TILs across ProMisE classifier subtypes. (G-I): CD94+, TIM-3+, TIGIT+, LAG-3+, Ki-67+, CD39+, CD103+CD39+, TCF-1+, and TOX+cells in CD8+ TILs across ProMisE classifier subtypes. *$p < 0.05$; **$p < 0.01$.

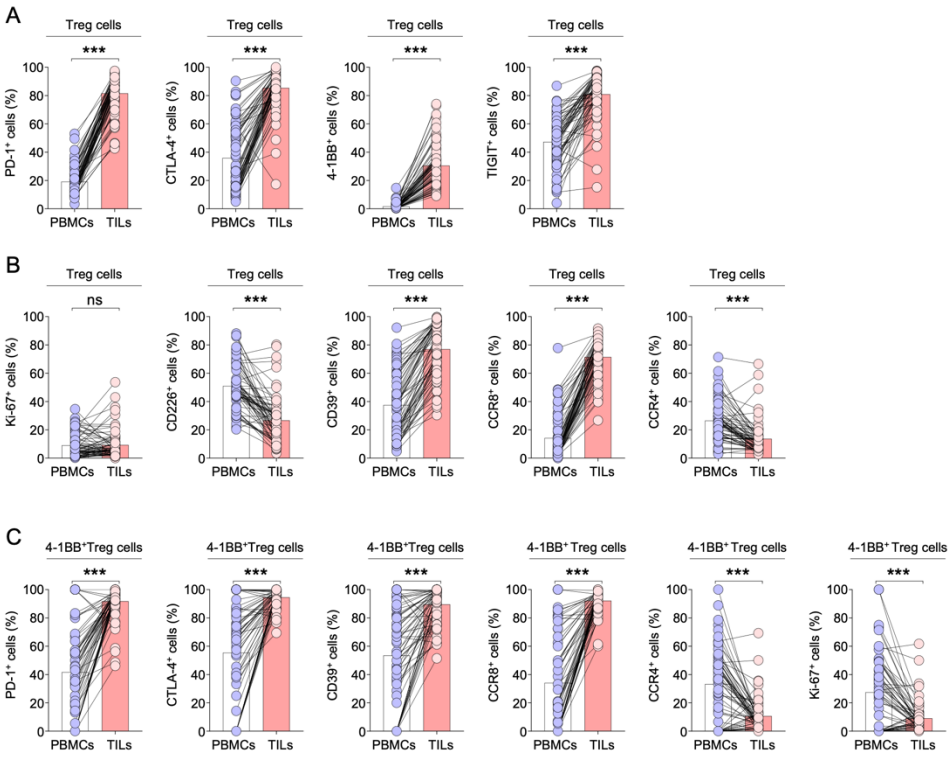

Figure 8. Tregs in PBMCs and TILs. (A) Comparison of PD-1+, CTLA-4+, 4-1BB+, TIGIT+ Tregs between PBMCs and TILs. (B) Expression of TIGIT+, Ki-67+, CD39+, CCR8+, and CCR4+ in Tregs from PBMCs and TILs. (C) PD-1+ and CTLA-4+ 4-1BB+ Tregs in PBMCs and TILs. ***p < 0.001.

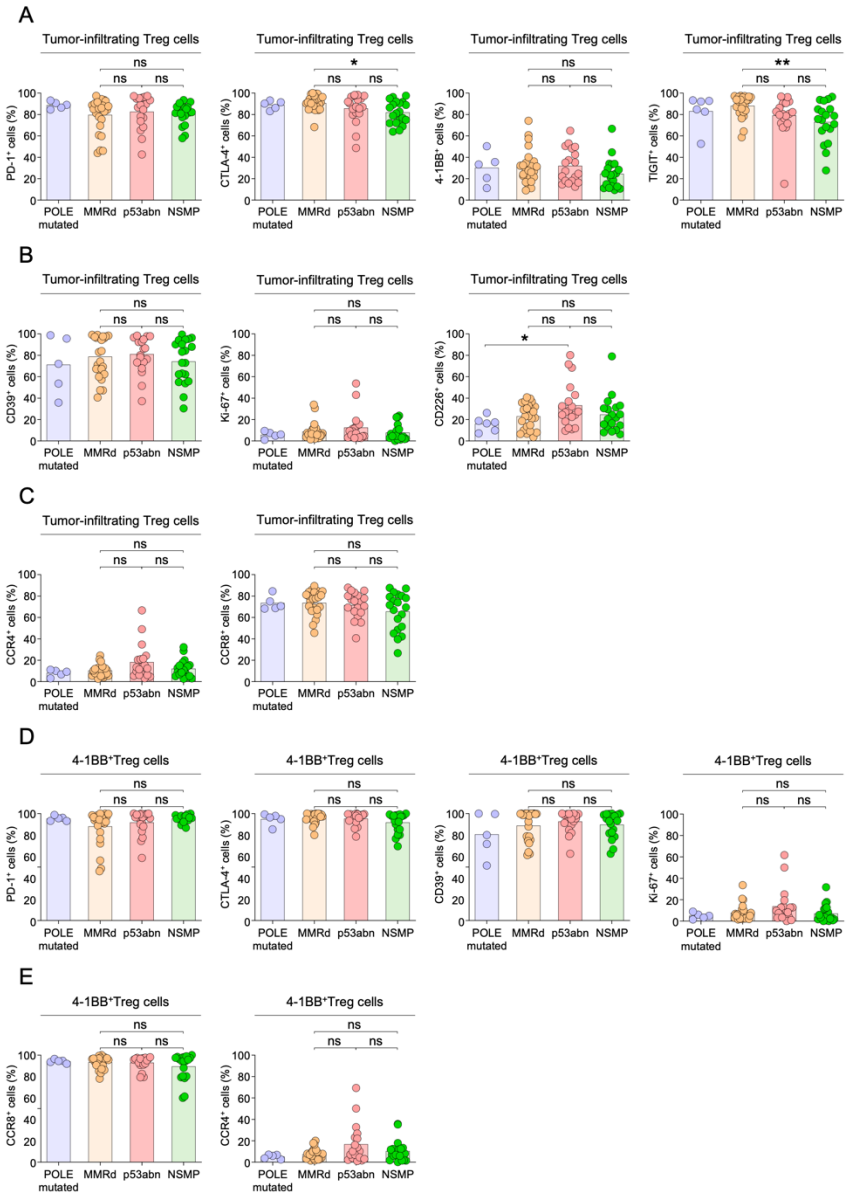

Figure 9. Tumor-infiltrating Tregs according to ProMisE classifier. (A-C) Expression of PD-1+, CTLA-4+, 4-1BB+, TIGIT+, CD39+, and CD226+ tumor-infiltrating Tregs across molecular subtypes. (D-E) Expression of PD-1+, CTLA-4+, CD39+, Ki-67+, CCR8+, and CCR4+ tumor-infiltrating 4-1BB+ Tregs across molecular subtypes. *p < 0.05; **p < 0.01.

3-6. Ex vivo anti-PD-1 response according to ProMisE classifier

We observed that aPD-1 treatment significantly increased CD8+ TIL proliferation and cytokine production, particularly IFN-γ and TNF-α, indicating strong immune activation (Figure 10). POLE-mutated and MMRd subtypes exhibited stronger responses, characterized by higher CD8+ T cell expansion, probably owing to their higher mutation burdens. Conversely, the p53abn and NSMP subtypes displayed weaker immune responses, with lower TIL infiltration and reduced cytokine production. These subtypes also showed a more immunosuppressive environment, suggesting resistance to PD-1 blockade. These findings indicate that the effectiveness of PD-1 inhibition varies by subtype, with POLE-mutated and MMRd subtypes likely deriving greater benefit from aPD-1 immunotherapy, while NSMP and p53-abnormal subtypes might necessitate alternative therapeutic strategies.

3-7. Distinct immune activation and exhaustion patterns in MSH2/MSH6-deficient EC subtypes

MSH2/MSH6-deficient tumors showed a higher proportion of effector memory CD8+ T cells and tumor-reactive CD8+ T cells, characterized by increased CD39 and CD103 co-expression, Tfh cells, and decreased expression of CD226+ and TCF+, than MLH1/PMS2-deficient tumors (Figure 11). Furthermore, increased numbers of CXCR5+PD-1+ CD8+ T cells and CD101+PD-1+ CD8+ T cells were observed in MSH2/MSH6-deficient tumors, indicating that this group may have a more pronounced T cell exhaustion profile than MLH1/PMS2-deficient tumors. However, markers associated with immune exhaustion, such as CTLA-4 and TIGIT, were not differentially expressed in Tregs in either group, except for PD-1 (Figure 12). These findings suggest distinct immune landscapes within different MMRd subtypes, with implications for targeted immunotherapies, such as PD-1 inhibitors, based on the immune profiles of both subgroups.

3-8. L1CAM-positive NSMP tumors exhibit elevated T cell exhaustion and immunosuppression, limiting response to PD-1 blockade

L1CAM-positive NSMP tumors were associated with significant changes in CD8+ TIL populations, particularly those linked to T cell exhaustion and immune suppression. PD-1^{high} CD8+ TILs, characteristic of T cell exhaustion, were significantly elevated in L1CAM+ tumors (Figure 13). Additionally, TIGIT+ and CD39+ CD8+ TILs, which are markers often associated with immune

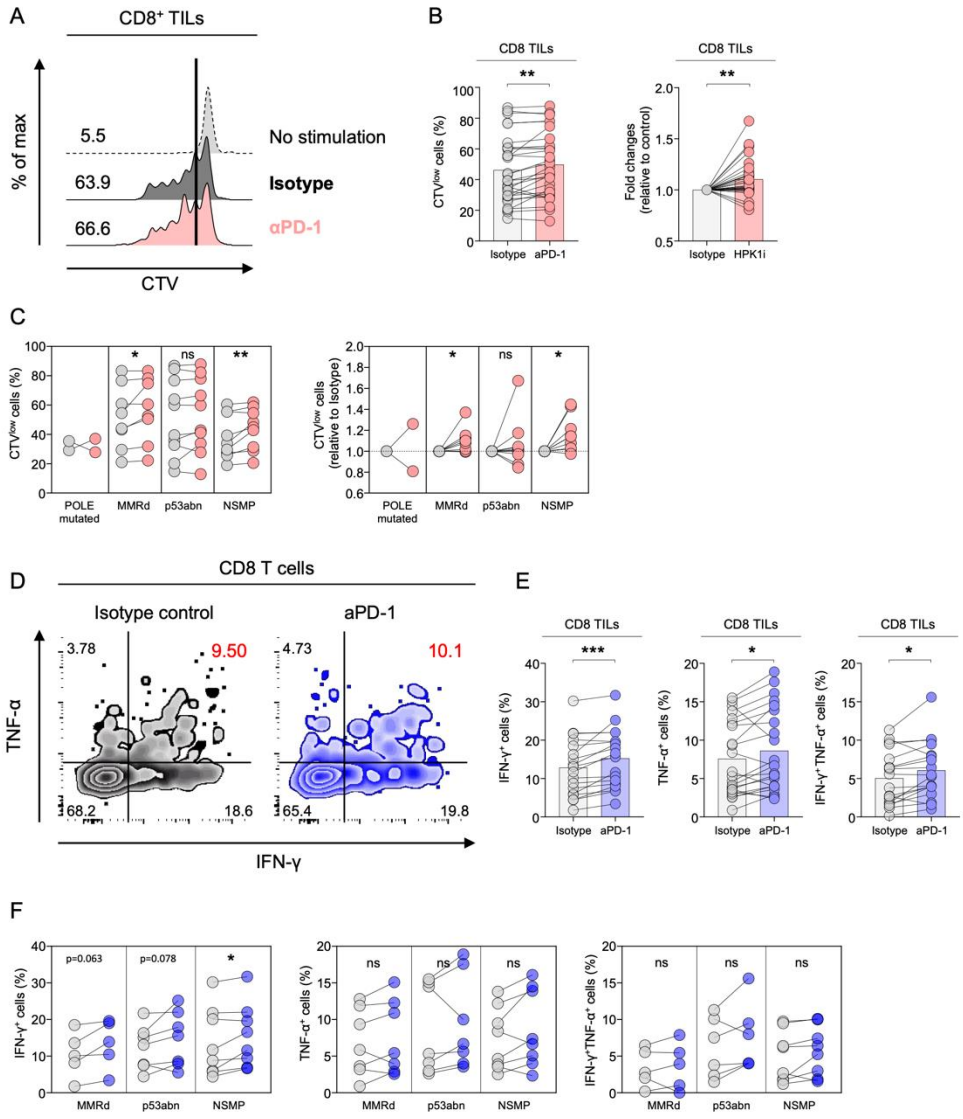

Figure 10. Ex vivo aPD-1 response according to ProMisE classifier. (A, B) Increase in the proportion of low-CTV cells, fold change following PD-1 Treatment in CD8+ TILs. (C) Comparison of low-CTV cells across molecular subtypes. (D) Increase in IFN-γ- and TNF-α-producing CD8+ TILs with PD-1 treatment. (E) Significant Increase in IFN-γ- and TNF-α -producing CD8+ TILs post PD-1 treatment. (F) Ex vivo aPD-1 response across ProMisE molecular subtypes. *p < 0.05; **p < 0.01; ***p < 0.001.

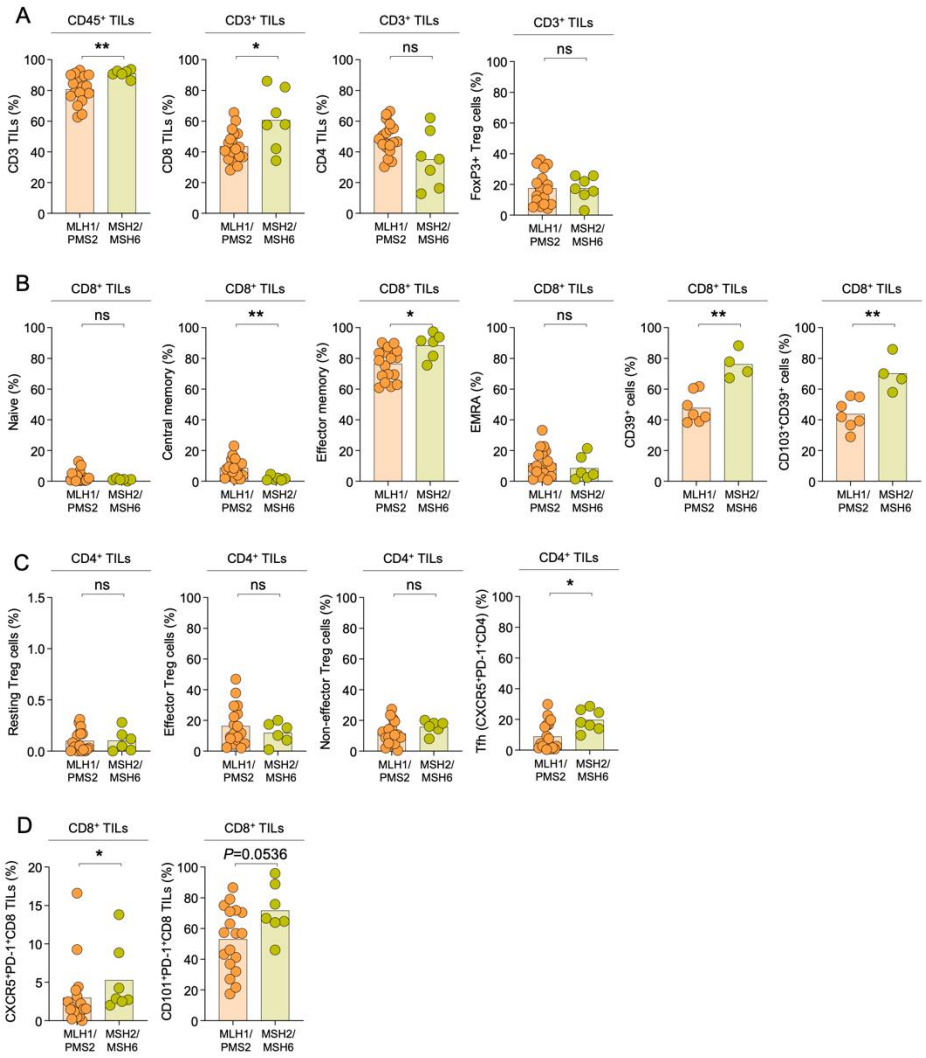

Figure 11. Cell composition of TILs according to MMRd subtypes. (A) Comparison of the proportions of CD4+ and CD8+ TILs across different MMRd subtypes. (B) Naive, memory, effector memory, EMRA, CD39+, and CD103+CD39+ CD8+ T cell subsets according to MMRd subtypes. (C) Comparison of resting, effector, non-effector Tregs, and Tfh across MMRd subtypes. (D) CXCR5+PD-1+ and CD101+PD-1+ CD8+ T cells according to MMRd subtypes. *p < 0.05; **p < 0.01.

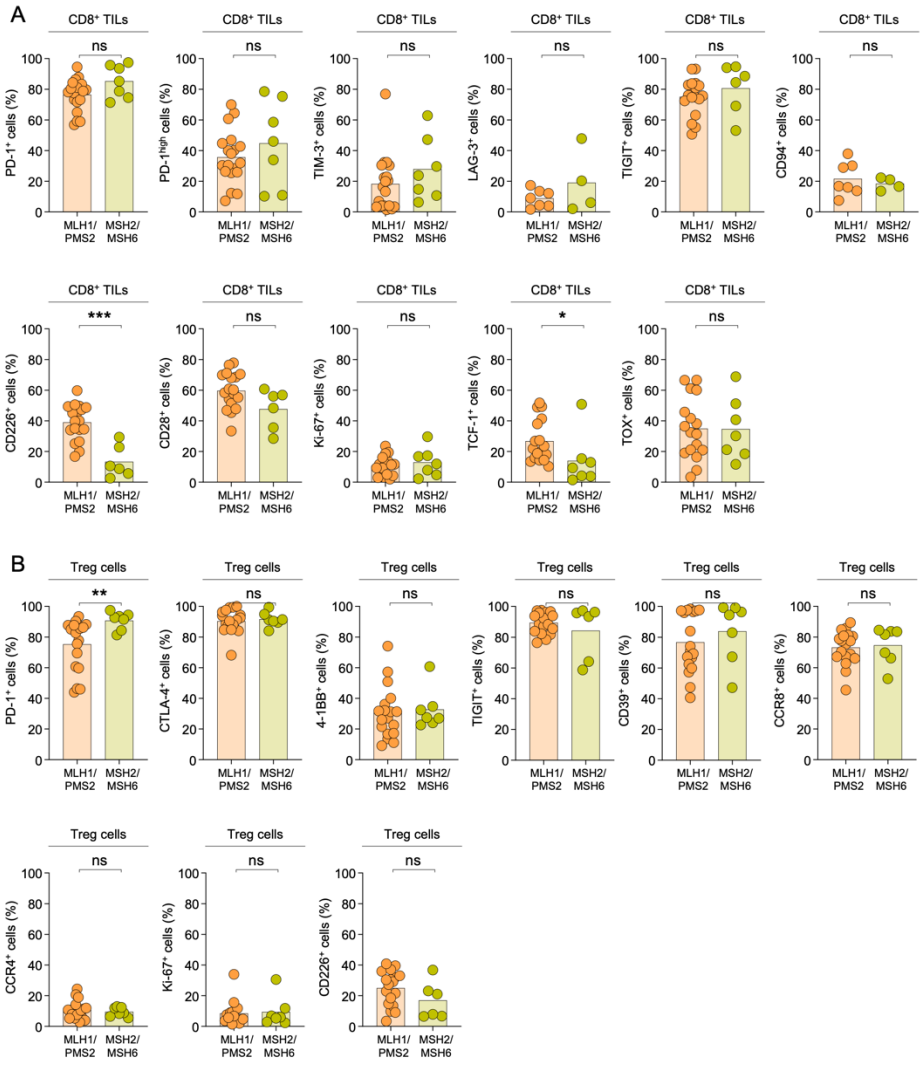

Figure 12. CD8+ TILs and Tregs according to MMRd subtypes. (A) Expression of PD-1+, PD-1+^{high}, TIM-3+, LAG-3+, TIGIT+, CD94+, CD226+, CD28+, Ki-67+, TCF-1+, and TOX+ TILs in CD8+ T cells. (B) Expression of PD-1+, TIGIT+, CTLA-4+, 4-1BB+, CD39+, CCR4+, Ki-67+, CD226+, and CCR8+ TILs in Tregs. *p < 0.05; **p < 0.01.

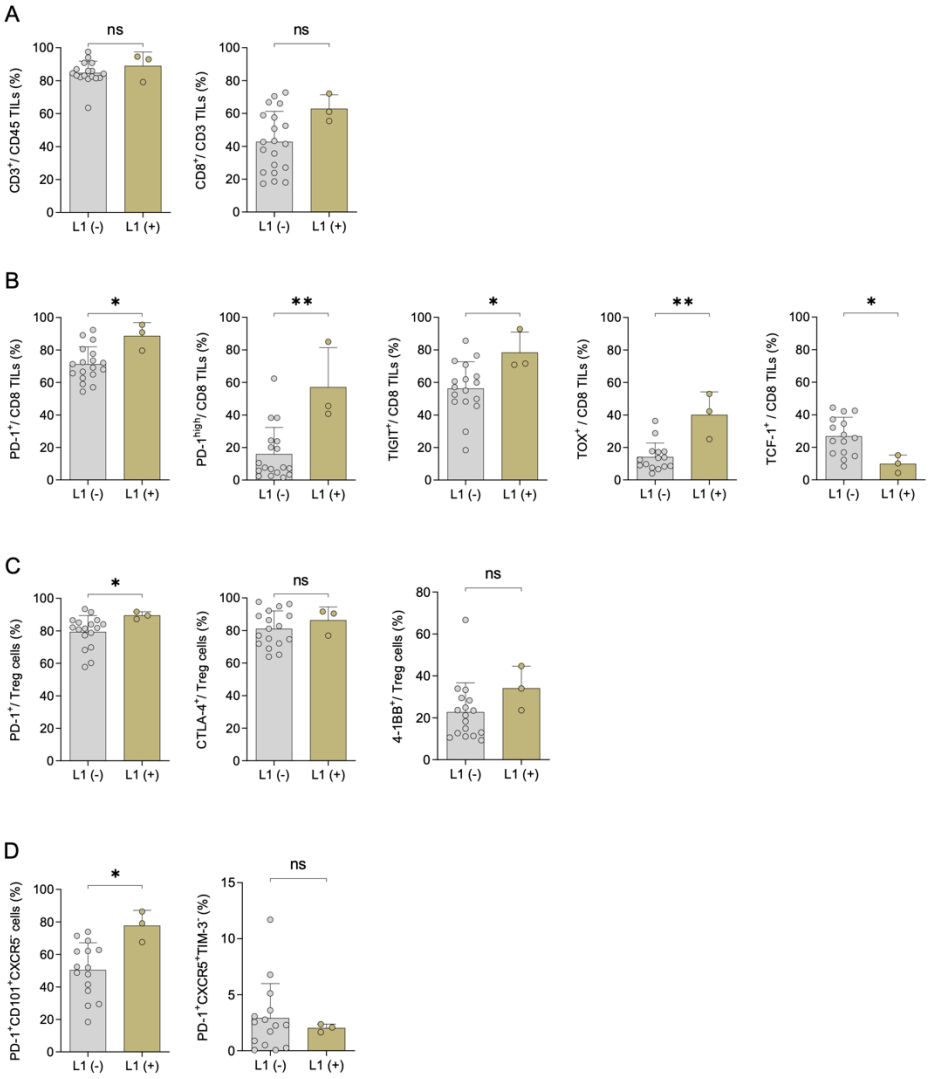

Figure 13. CD8+ TILs according to L1CAM presentation in NSMP subtypes. (A) Proportion of TILs during L1CAM presentation. (B) Expression of PD-1+, PD-1^{high}, TIGIT+, TOX+, and TCF-1+ CD8+ TILs during L1CAM presentation. (C) Expression of PD-1+, CTLA-4+, and 4-1BB+ tumor-infiltrating Tregs during L1CAM presentation. (D) Distribution of PD-1+CD101+CXCR5- TILs during L1CAM presentation. *p < 0.05; **p < 0.01; *L1(-)*, L1CAM negative; *L1(+)*, L1CAM positive.

suppression and regulatory functions in the tumor microenvironment, increased notably. These cells typically elicit a less effective immune response because of their involvement in inhibitory signaling pathways that prevent T cell activation and proliferation. Furthermore, TOX+ CD8+ TILs—another marker of exhausted T cells— was also increased in L1CAM-positive tumors, reinforcing that these tumors exhibit a microenvironment conducive to T cell exhaustion. A reduction in TCF-1+ CD8+ TILs was observed, indicating depletion of T cells with self-renewing potential. TCF-1 is crucial for maintaining T cell memory and sustained antitumor activity. Therefore, the lower frequency of TCF-1+ cells in L1CAM-positive tumors suggests that these tumors are less capable of sustaining long-term immune responses. In addition to these changes in the CD8+ TIL population, the analysis showed a significant increase in PD-1+ Tregs in L1CAM-positive tumors. Tregs suppress the immune response, further contributing to an immunosuppressive microenvironment. Additionally, the number of PD-1+CD101+CXCR5+ cells, which may represent exhausted Tfh cells or other regulatory subsets, was elevated, indicating a suppressed immune response in these tumors. This combination of exhausted CD8+ T cells and elevated Tregs points to a highly immunosuppressive tumor microenvironment in L1CAM-positive NSMP tumors, which may limit the efficacy of immune checkpoint blockade therapies, such as aPD-1.

3-9. Distinct immune profile of *ARID1A*-negative NSMP tumors

ARID1A-negative NSMP tumors exhibited a different immune landscape with distinct characteristics that may influence their response to immunotherapy (Figure 14). These tumors showed increased levels of PD-1 ^{high} CD8+ TILs, TIGIT+ CD8+ TILs, and CD39+ CD8+ TILs, indicating some degree of T cell exhaustion. These cells play a crucial role in local immune surveillance and are often associated with highly effective tumor immune escape. The presence of activated immunosuppressive T cells in this tumor subtype suggests that these tumors may exhibit a favorable immune profile for response to immunotherapies, particularly those targeting immune checkpoints, such as PD-1.

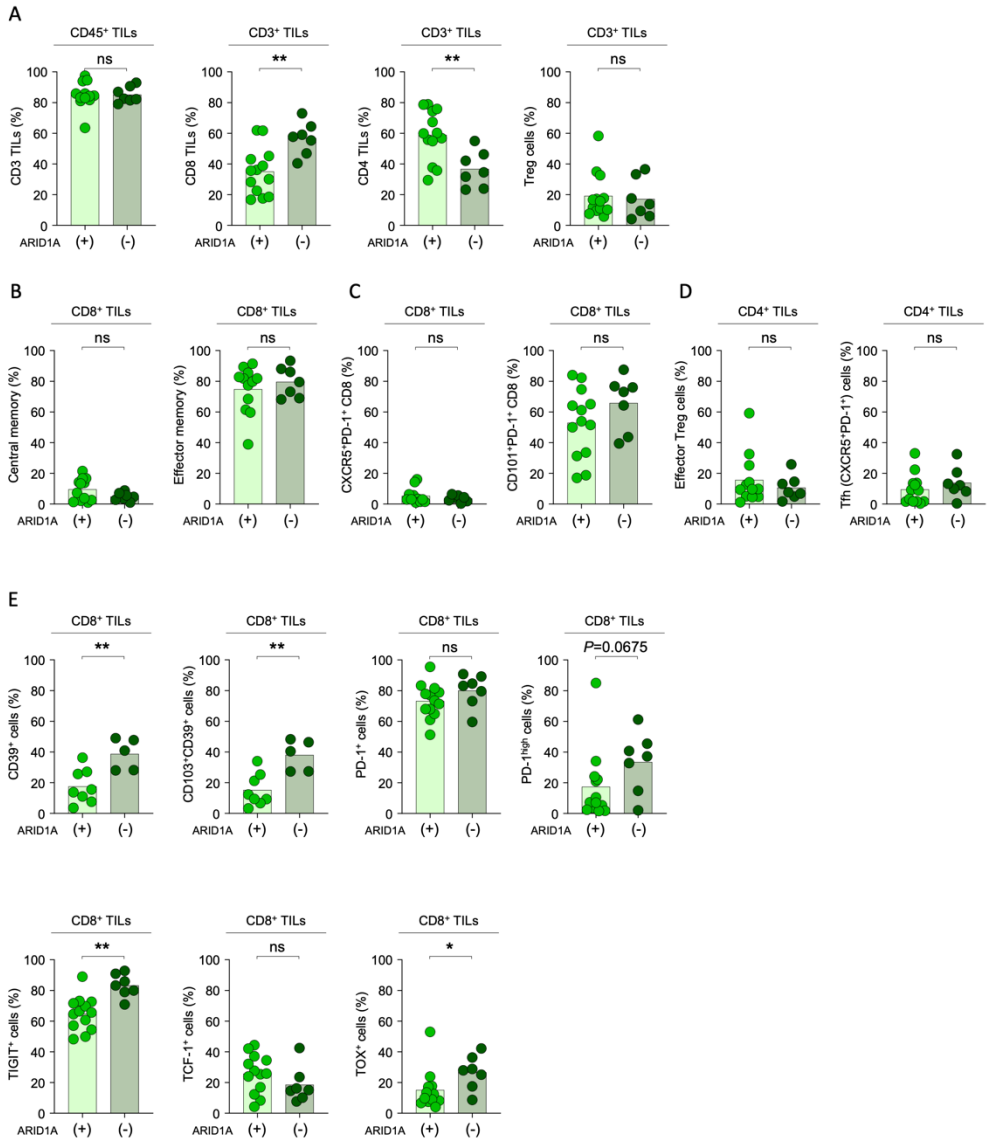

Figure 14. CD8+ TILs according to *ARID1A* presentation in NSMP subtypes. (A) Proportion of CD8, CD4, Treg TILs in *ARID1A* presentation. (B, C) Distribution of central memory. effector memory, CXCR5+PD-1+, CD101+PD-1+ CD8+ TILs in *ARID1A* presentation. (D) Expression of effector Tregs, Tfh cells in *ARID1A* presentation. (E) Expression of CD39+, CD103+CD39+, PD-1+, PD-1high+, TIGIT, TCF-1+, TOX+ TIL in *ARID1A* presentation. *p<0.05; **p<0.01.

4. DISCUSSION

The distinct immune profiles observed across ProMisE subtypes highlight the importance of molecular classification in informing treatment decisions for EC.

The POLE-mutated and MMRd subtypes, characterized by a robust yet exhausted immune response, exhibited elevated levels of PD-1+, TIM-3+, TOX+, CD39+, and CD103+CD39+ cells. The levels of these markers suggest a highly active yet immunosuppressed environment and an immunosuppressive environment that may be targeted by ICIs.

TCF-1, which was lower in the MMRd subtype, plays a vital role in maintaining T cell functionality and preventing full exhaustion. As a master regulator, TCF-1 is essential for maintaining the less-exhausted, stem-like subset of CD8+ T cells that possess self-renewal potential and long-term persistence. Thus, this subset is a key responder to immune checkpoint therapies, such as anti-PD-1/PD-L1 blockade [19]. TCF-1 is involved in the regulation of CD8+ T cells by driving the expression of effector-associated genes and promoting a balanced state that prevents terminal exhaustion [20]. This regulatory role is crucial in MMRd tumors, where TCF-1 expression is related with enhanced responses to ICIs. Moreover, TCF-1 expression in CD8+ T cells prevents apoptosis and supports the development of memory-like phenotypes that sustain antitumor immune responses over time, making it a promising biomarker for determining responsiveness to immunotherapies [19].

The role of TCF-1 in the regulation of immune responses has gained increasing attention in the field of cancer immunotherapy. In a study by Siddiqui et al., which indicated that TCF-1+ cells possess an increased responsiveness to PD-1 inhibition due to their capacity to differentiate into cytotoxic effector cells, underscoring their potential contribution to shaping long-term immune responses [21].

Khan et al. emphasized the importance of TCF-1 in maintaining a pool of memory-like CD8+ T cells, which may persist in a less-exhausted state, during chronic viral infections and cancers [22]. These TCF-1+ cells act as reservoirs for cells capable of responding to subsequent immune challenges, thereby enhancing the durability of immune responses in cancer therapy. The low presence of TCF-1+CD8+ T cells in MMRd subtype tumors, as seen in our study, may explain its

heightened responsiveness to ICIs, despite the presence of exhaustion markers, such as TOX and PD-1.

Therapies that promote TCF-1 activity have been combined with immune checkpoint inhibition to further enhance T cell reinvigoration. Utzschneider et al. reported that the upregulation of TCF-1 could synergize with PD-1 blockade to reinvigorate exhausted T cells and promote sustained antitumor immunity [23].

TIGIT is an emerging immune checkpoint that has gained attention because of its role in T and NK cell inhibition via interactions with its ligands CD155 and CD112 [24]. The upregulation of TIGIT in MMRd tumors, particularly in Tregs, suggests an added layer of immune suppression, as TIGIT prevents effective T cell-mediated antitumor responses. Harjunpää et al. highlighted that TIGIT expression correlates with T cell exhaustion, and blocking TIGIT can restore effector T cell function and enhance responses to PD-1 blockade [25]. In a study by Chauvin et al., the combination of anti-TIGIT (aTIGIT) and aPD-1 therapies significantly improved tumor control in melanoma models [26]. Based on this results of these studies, TIGIT blockade may be combined with PD-1 or CTLA-4 inhibition for treating MMRd EC in clinical settings.

MMRd subtype tumors showed the most pronounced response to aPD-1 therapy, with a marked increase in CD8+ T cell proliferation and cytokine production, particularly those of IFN-γ and TNF-α. MMRd tumors, owing to their high mutational burden, are highly immunogenic, responsive to ICIs, and show significant benefits from PD-1 blockade [27].

Conversely, the p53abn and NSMP subtype tumors exhibited weaker responses, probably because of their lower immunogenicity. KEYNOTE-158 trial confirmed that MMRd tumors have better objective response rates than that of p53abn and NSMP subtype tumors [28]. This suggests the need for combining ICIs with agents, such as PARP inhibitors or chemotherapy for p53abn and NSMP subtype tumors to enhance the effectiveness of treatment and identify new therapeutic strategies.

MMRd EC and MMRd colorectal cancer (CRC) exhibit several similarities. Both these cancers exhibit a high tumor mutational burden, MSI-H, and enhanced expression of neoantigens, leading to a robust antitumor immune response characterized by increased infiltration of CD8+ T cells and upregulation of immune checkpoint markers, such as PD-1 and PD-L1 [29]. However, differences emerge in the composition and activity of TILs and the tumor microenvironment. The immune responses in MMRd CRC are more organized and compartmentalized than that in MMRp CRC, often with spatially segregated immune hubs that facilitate enhanced immune coordination and

cytotoxic activity; this has not been previously observed in MMRd EC [30].

These findings suggest that approaches proven successful in MMRd CRC, such as targeting specific T cell subsets or modulating T cell exhaustion pathways, could be translated into MMRd EC research. For instance, combining PD-1 blockade with therapies targeting TIGIT or CD39, which have shown efficacy in MMRd CRC, could be tested in MMRd EC [31]. By targeting these shared and unique pathways, treatment strategies can be tailored to the distinct immunological contexts of each cancer type.

The combination of aCTLA-4 drugs, such as ipilimumab and tremelimumab with other ICIs, such as PD-1 blockers is effective in CRC, particularly in subtypes that are resistant to monotherapy. For example, the CheckMate-142 trial demonstrated a 55% objective response rate and an 80% disease control rate with nivolumab and ipilimumab, leading to its FDA approval in 2018 [32]. Furthermore, CTLA-4 expression in Tregs was significantly elevated in the MMRd group, in line with the findings from our study. In addition, real-world clinical trials are currently underway to investigate the application of ipilimumab and nivolumab in advanced MMRd EC, highlighting the importance of these results [33]. Additionally, combining aTIGIT agents, such as vibostolimab, with other therapies to modulate Tregs may be a promising strategy, and the outcomes of such trials are highly anticipated [34].

In advanced CRC with MMRd status, prognosis remains poor despite targeted therapies. Venderbosch et al. demonstrated that patients with MMRd tumors had lower PFS and OS than those with MMRp tumors. Furthermore, they reported that BRAF mutations were associated with poorer outcomes in MMRp tumors, however, had no impact on prognosis in MMRd tumors, highlighting the prognostic differences in the role of BRAF depending on MMR status [35]. However, data from the ACCENT group indicated that MMRd tumors exhibited better outcomes than MMRp tumors, regardless of BRAF mutation status [36, 37]. These discrepancies underscore the need for further investigation into the role of MMRd status in EC and immunological mechanisms underlying these differences to explain the observed prognostic variations.

Comparison between the MLH1/PMS2 and MSH2/MSH6 subgroups within MMRd EC revealed important differences in immune infiltration and T cell activity. Notably, MSH2/MSH6-deficient tumors exhibited significantly higher CD8+ T cell infiltration than MLH1/PMS2-deficient tumors, suggesting a more active antitumor immune response in the MSH2/MSH6-deficient group. Further corroborating this finding, MSH2/MSH6 mutations led to increased neoantigen loads and immune

infiltration, making these tumors highly responsive to ICIs [38-40]. The presence of CD39 in TILs is increasingly being recognized as a marker of immune exhaustion, particularly in tumors and promoted tumors growth [41]. Additionally, the reduced expression of TCF-1+ CD8+ TILs in these tumors suggests a diminished reservoir of stem-like T cells, which is crucial for sustained responses to immunotherapy [42]. Thus MSH2/MSH6-deficient tumors may respond well to ICIs. Furthermore, CD39+ CD103+ TILs, which are enriched with MSH2/MSH6-deficient tumors, are often associated with a good response to ICIs [43]. This suggests that patients with these mutations may benefit from combination therapies aimed at mitigating T cell exhaustion, such as targeting the adenosine pathway or using anti-CD39 antibodies.

The upregulation of exhaustion markers, such as PD-1, TIGIT, CD39, and TOX, in CD8+ TILs in the L1CAM-positive NSMP subtype suggests that L1CAM-positive tumors harbor a more exhausted immune microenvironment than that by L1CAM-negative tumors. Moreover, the decreased frequency of TCF-1+ CD8+ TILs in L1CAM-positive tumors further supports the presence of a more terminally exhausted T cell population. TCF-1 is a crucial marker of progenitor-exhausted T cells, which retain their capacity for reinvigoration and are necessary for a sustained response to ICI therapy [42]. The lower prevalence of L1CAM-positive tumors among patients suggests a limited reservoir of T cells capable of responding to treatment, potentially contributing to the poor prognosis in this group. Additionally, increased infiltration of CD101+ CD8+ TILs, a marker of terminally exhausted cells, in L1CAM-positive tumors indicates that these tumors may be less responsive to conventional immunotherapy [44].

Enhanced expression of PD-1 and TIGIT in *ARID1A*-mutated tumors indicates an immunosuppressive microenvironment that potentially leads to immune evasion. TOX, a transcription factor that regulates T cell exhaustion, is crucial for maintaining the exhausted phenotype of TILs [45]. Furthermore, CD39+ T cells, which are associated with the generation of immunosuppressive adenosines, may exacerbate the immunosuppressive environment [41]. We observed a reduction in the number of TCF-1+ CD8+ TILs with *ARID1A* mutations. These results suggest a limited reservoir of functional T cells in *ARID1A* mutations, which further complicates the efficacy of ICIs in these patients [42]. Overall, our findings indicated that *ARID1A* mutations contribute to an immunosuppressive environment characterized by terminal T cell exhaustion. These insights suggest that *ARID1A*-negative EC may benefit from combination therapies aimed at

reversing T cell exhaustion or targeting immunosuppressive pathways, such as aPD-1 or anti-CD39 treatments.

5. CONCLUSION

This study revealed distinct immune profiles across the EC molecular subtypes, emphasizing the therapeutic relevance of these differences. The POLE-mutated and MMRd subtypes showed robust, however, exhausted immune responses, marked by elevated PD-1, TOX, and TIM-3 expression levels, suggesting their suitability for ICI therapy. Conversely, the p53abn and NSMP subtypes exhibited immunosuppressive microenvironments with low T cell infiltration, indicating reduced responsiveness to immunotherapy. The MSH2/MSH6-deficient group showed higher CD8+ T cell infiltration and immune activity than the MLH1/PMS2-deficient group, highlighting the potential for enhanced responses to ICI therapy. Additionally, L1CAM-positive NSMP tumors showed increased T cell exhaustion and immune suppression, and *ARID1A*-negative tumors exhibited a slightly less favorable immune profile with fewer tissue-resident memory T cells, suggesting that these tumors may respond poorly to tailored immunotherapies targeting T cell exhaustion pathways. These findings underscore the importance of molecular subtyping for optimizing immunotherapy strategies for patients with EC.

REFERENCES

1. Wortman, B.G., et al., *Selecting Adjuvant Treatment for Endometrial Carcinoma Using Molecular Risk Factors.* Curr Oncol Rep, 2019. **21**(9): p. 83.
2. National Cancer Center, M.o.H. and Welfare, *Annual Report of Cancer Statistics in Korea in 2021.* 2023.
3. Ruan, H., et al., *Development and Validation of a Nomogram Prediction Model for Endometrial Malignancy in Patients with Abnormal Uterine Bleeding.* Yonsei Med J, 2023. **64**(3): p. 197-203.
4. National Comprehensive Cancer, N., *NCCN Clinical Practice Guidelines in Oncology (NCCN Guidelines®) Endometrial Cancer Version 1.2024.* 2024.
5. Chang, K., et al., *The Cancer Genome Atlas Pan-Cancer analysis project.* Nature Genetics, 2013. **45**(10): p. 1113-1120.
6. Talhouk, A., et al., *Confirmation of ProMisE: A simple, genomics-based clinical classifier for endometrial cancer.* Cancer, 2017. **123**(5): p. 802-813.
7. Wortman, B.G., et al., *Ten-year results of the PORTEC-2 trial for high-intermediate risk endometrial carcinoma: improving patient selection for adjuvant therapy.* Br J Cancer, 2018. **119**(9): p. 1067-1074.
8. Levine, D.A., et al., *Integrated genomic characterization of endometrial carcinoma.* 2013. **497**(7447): p. 67-73.
9. Gómez-Raposo, C., et al., *Immune checkpoint inhibitors in endometrial cancer.* Critical Reviews in Oncology/Hematology, 2021. **161**: p. 103306.
10. Kim, M., et al., *Rechallenge with Anti-PD-1 Inhibitors in Patients with Recurrent Gynecologic Malignancies.* Yonsei Med J, 2023. **64**(10): p. 587-592.
11. Xing, T., et al., *ARID1A deficiency promotes progression and potentiates therapeutic antitumour immunity in hepatitis B virus-related hepatocellular carcinoma.* BMC Gastroenterology, 2024. **24**(1): p. 11.
12. Mandal, J., et al., *Treating ARID1A mutated cancers by harnessing synthetic lethality and DNA damage response.* Journal of Biomedical Science, 2022. **29**(1): p. 71.
13. Sun, D., et al., *ARID1A deficiency reverses the response to anti-PD(L)1 therapy in EGFR-mutant lung adenocarcinoma by enhancing autophagy-inhibited type I interferon production.* Cell Communication and Signaling, 2022. **20**(1): p. 156.

14. Giordano, M., et al., *L1CAM promotes ovarian cancer stemness and tumor initiation via FGFR1/SRC/STAT3 signaling.* Journal of Experimental & Clinical Cancer Research, 2021. **40**(1): p. 319.
15. Wolterink, S., et al., *Therapeutic antibodies to human L1CAM: functional characterization and application in a mouse model for ovarian carcinoma.* Cancer Res, 2010. **70**(6): p. 2504-15.
16. Grage-Griebenow, E., et al., *L1CAM promotes enrichment of immunosuppressive T cells in human pancreatic cancer correlating with malignant progression.* Molecular oncology, 2014. **8**(5): p. 982-997.
17. Dobin, A., et al., *STAR: ultrafast universal RNA-seq aligner.* Bioinformatics, 2013. **29**(1): p. 15-21.
18. Liao, Y., G.K. Smyth, and W. Shi, *featureCounts: an efficient general purpose program for assigning sequence reads to genomic features.* Bioinformatics, 2013. **30**(7): p. 923-930.
19. Jung, S. and J.H. Baek, *The Potential of T Cell Factor 1 in Sustaining CD8(+) T Lymphocyte-Directed Anti-Tumor Immunity.* Cancers (Basel), 2021. **13**(3).
20. Roetman, J.J., et al., *Tumor-Reactive CD8+ T Cells Enter a TCF1+PD-1- Dysfunctional State.* Cancer Immunol Res, 2023. **11**(12): p. 1630-1641.
21. Siddiqui, I., et al., *Intratumoral Tcf1(+)PD-1(+)CD8(+) T Cells with Stem-like Properties Promote Tumor Control in Response to Vaccination and Checkpoint Blockade Immunotherapy.* Immunity, 2019. **50**(1): p. 195-211.e10.
22. Khan, O., et al., *TOX transcriptionally and epigenetically programs CD8⁺ T cell exhaustion.* Nature, 2019. **571**(7764): p. 211-218.
23. Utzschneider, D.T., et al., *T Cell Factor 1-Expressing Memory-like CD8(+) T Cells Sustain the Immune Response to Chronic Viral Infections.* Immunity, 2016. **45**(2): p. 415-27.
24. Seel, K., et al., *Blockade of the TIGIT-CD155/CD112 axis enhances functionality of NK-92 but not cytokine-induced memory-like NK cells toward CD155-expressing acute myeloid leukemia.* Cancer Immunol Immunother, 2024. **73**(9): p. 180.
25. Harjunpää, H. and C. Guillerey, *TIGIT as an emerging immune checkpoint.* Clin Exp Immunol, 2020. **200**(2): p. 108-119.
26. Chauvin, J.M., et al., *TIGIT and PD-1 impair tumor antigen-specific CD8$^+$ T cells in melanoma patients.* J Clin Invest, 2015. **125**(5): p. 2046-58.
27. Le, D.T., et al., *PD-1 Blockade in Tumors with Mismatch-Repair Deficiency.* N Engl J Med, 2015. **372**(26): p. 2509-20.
28. Marabelle, A., et al., *Efficacy of Pembrolizumab in Patients With Noncolorectal High Microsatellite Instability/Mismatch Repair-Deficient Cancer: Results From the Phase II KEYNOTE-158 Study.* J Clin Oncol, 2020. **38**(1): p. 1-10.

29. Naboush, A., C.A.J. Roman, and I. Shapira, *Immune checkpoint inhibitors in malignancies with mismatch repair deficiency: a review of the state of the current knowledge.* Journal of Investigative Medicine, 2017. **65**(4): p. 754.
30. Pelka, K., et al., *Spatially organized multicellular immune hubs in human colorectal cancer.* Cell, 2021. **184**(18): p. 4734-4752.e20.
31. Westcott, P.M.K., et al., *Mismatch repair deficiency is not sufficient to elicit tumor immunogenicity.* Nature Genetics, 2023. **55**(10): p. 1686-1695.
32. Lenz, H.J., et al., *First-Line Nivolumab Plus Low-Dose Ipilimumab for Microsatellite Instability-High/Mismatch Repair-Deficient Metastatic Colorectal Cancer: The Phase II CheckMate 142 Study.* J Clin Oncol, 2022. **40**(2): p. 161-170.
33. *A Randomized Phase II Trial of Nivolumab and Ipilimumab Compared to Nivolumab Monotherapy in Patients With Deficient Mismatch Repair System Recurrent Endometrial Carcinoma*, N.R.G. Oncology, Editor. 2021.
34. Rojas, C., et al., *Vibostolimab coformulated with pembrolizumab (vibo/pembro) for previously treated advanced mismatch repair–deficient (dMMR) endometrial cancer: Results from cohort B1 of the phase 2 KEYVIBE-005 study.* Journal of Clinical Oncology, 2024. **42**(16_suppl): p. 5502-5502.
35. Venderbosch, S., et al., *Mismatch repair status and BRAF mutation status in metastatic colorectal cancer patients: a pooled analysis of the CAIRO, CAIRO2, COIN, and FOCUS studies.* Clin Cancer Res, 2014. **20**(20): p. 5322-30.
36. Taieb, J., et al., *Prognosis of microsatellite instability and/or mismatch repair deficiency stage III colon cancer patients after disease recurrence following adjuvant treatment: results of an ACCENT pooled analysis of seven studies.* Annals of Oncology, 2019. **30**(9): p. 1466-1471.
37. Taieb, J., et al., *Deficient mismatch repair/microsatellite unstable colorectal cancer: Diagnosis, prognosis and treatment.* European Journal of Cancer, 2022. **175**: p. 136-157.
38. Pritchard, C.C., et al., *Complex MSH2 and MSH6 mutations in hypermutated microsatellite unstable advanced prostate cancer.* Nat Commun, 2014. **5**: p. 4988.
39. Zhao, P., et al., *Mismatch repair deficiency/microsatellite instability-high as a predictor for anti-PD-1/PD-L1 immunotherapy efficacy.* J Hematol Oncol, 2019. **12**(1): p. 54.
40. Zhou, L.Z., H.Q. Xiao, and J. Chen, *Mismatch repair gene MSH6 correlates with the prognosis, immune status and immune checkpoint inhibitors response of endometrial cancer.* Front Immunol, 2024. **15**: p. 1302797.
41. Vijayan, D., et al., *Targeting immunosuppressive adenosine in cancer.* Nature Reviews Cancer, 2017. **17**(12): p. 709-724.

42. Im, S.J., et al., *Defining CD8+ T cells that provide the proliferative burst after PD-1 therapy.* Nature, 2016. **537**(7620): p. 417-421.
43. Simoni, Y., et al., *Bystander CD8(+) T cells are abundant and phenotypically distinct in human tumour infiltrates.* Nature, 2018. **557**(7706): p. 575-579.
44. Beltra, J.C., et al., *Developmental Relationships of Four Exhausted CD8(+) T Cell Subsets Reveals Underlying Transcriptional and Epigenetic Landscape Control Mechanisms.* Immunity, 2020. **52**(5): p. 825-841.e8.
45. Khan, O., et al., *TOX transcriptionally and epigenetically programs CD8(+) T cell exhaustion.* Nature, 2019. **571**(7764): p. 211-218.

Abstract in Korean

자궁내막암의 분자 유형별 면역 프로필과 치료 전략

목적

본 연구는 자궁내막암의 Proactive Molecular Risk Classifier for Endometrial Cancer (ProMisE) 분류에 따른 분자 유형별 면역 프로파일을 평가하고, DNA 불일치 복구 단백 결손(MMRd)의 아형 및 No Specific Molecular Profile (NSMP) 유형의 L1 cell adhesion molecule (L1CAM), AT-rich interaction domain 1A (*ARID1A*) 발현 양상에 따른 면역 반응과 치료 잠재력에 미치는 영향을 분석하고자 하였다.

방법

2019 년부터 2023 년까지 세브란스 산부인과 환자 중 처음 진단된 자궁내막암 환자를 대상으로 연구를 진행하였다. 분자 유형을 나누고 특정 표지자들을 확인하기 위해 POLE 돌연변이는 droplet digital PCR 을 통해 분석하였으며, 면역조직화학 염색법을 사용하여 p53, MMR 단백 (MSH6, PMS2, MSH2, MLH1), L1CAM, 및 *ARID1A* 의 발현을 평가하였다. 또한 면역 반응을 확인하고자 종양 침윤 림프구는 유세포 분석법을 이용하여 다양한 면역 세포 아형 및 이들의 기능적 상태 (CD8+ T 세포, 조절 T 세포, T 세포 피로 및 활성화 표지자 등)를 확인하였다.

결과

자궁내막암의 분자 유형에 따라 면역 프로파일이 다양하게 나타났다. POLE 돌연변이 및 MMRd 유형은 면역 피로 징후를 보이나 면역관문억제제에 강한 면역 반응을 보였다. NSMP 및 p53abnormal 유형은 낮은 면역 세포 침윤과 면역 억제 환경을 나타냈다. MSH2/MSH6 결손 유형은 MLH1/PMS2 결손 유형보다 높은 CD8+ T 세포 침윤을 보였으며, 이는 더 활발한 면역 반응을 시사하였다. NSMP 유형에서 L1CAM 양성일 경우 PD-1 및 TIGIT 과 같은 T 세포 피로 표지자가 증가하였다. 또한 NSMP 유형에서 *ARID1A* 음성일 경우 종양 특이적 T 세포(CD103+CD39+)가 많이 존재하며, 일부 면역 피로 징후 또한 관찰되었다.

결론

본 연구는 자궁내막암에서 개인 맞춤형 면역치료 전략을 수립하기 위해 분자 분류의 중요성을 강조한다. POLE 돌연변이 및 MMRd 유형은 강한 면역 반응을 보였으나, 면역 피로의 징후가 관찰되어 면역관문억제제에 대한 반응 가능성을 시사하였다. 또한, MSH2/MSH6 결손 종양, NSMP 유형의 L1CAM 양성, *ARID1A* 음성 유형은 면역 피로를 역전시키고 치료 결과를 개선하기 위한 새로운 치료 접근법의 잠재적 표적이 될 수 있다.

핵심되는 말 : 자궁내막암; 분자 유형; 종양 침윤 림프구